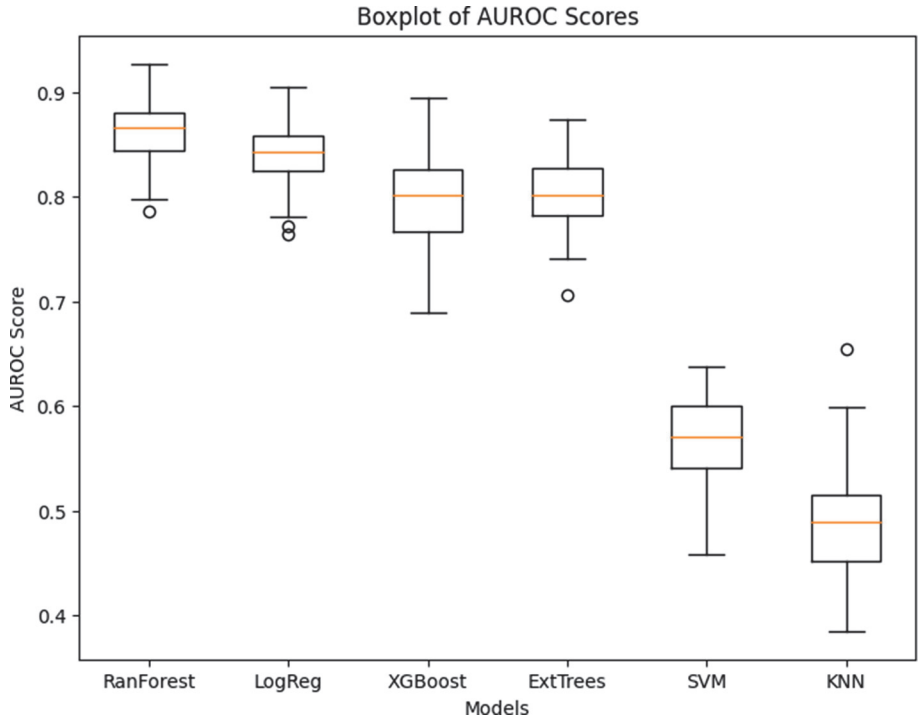

Abstract E-226 Figure 1

important reimbursement criterion. We assess the feasibility of machine learning to preoperatively predict NHD after unruptured intracranial aneurysm (UIA) treatment. Identifying patients at risk for NHD after UIA treatment could help guide providers that plan on counseling patients and help plan discharges for NHD patients.

Methods From a prospectively maintained database, all patients (n=547) treated for UIA between 2017 and 2022 was retrospectively reviewed. 21 baseline characteristics were collected, including age, sex, and underlying medical conditions. 7 UIA and treatment characteristics were also collected, including aneurysm morphology, location, modality of treatment (open surgery vs endovascular), and endovascular access route (radial, femoral). The data was randomly divided into training and testing sets with an 80:20 ratio. Given the unbalanced classes, Synthetic Minority Over-sampling TEchnique (SMOTE) was applied to the training set. Logistic regression and five machine learning algorithms were trained: Random Forest, Extremely Randomized Trees, Extreme Gradient Boosting (XGBoost), Support Vector Machine (SVM), and k-nearest neighbors (KNN).

Results 520 (95%) of eligible patients had no missing data and were selected for analysis. The rate of NHD was 3.8% (n=20). Random Forest was the best discriminant of NHD and had the highest mean AUROC of 0.86 (s.d. ±0.03) and accuracy of 0.93 (±0.01). Random Forest narrowly but significantly (Mann-Whitney U-test; p = 0.002) outperformed logistic regression which had AUROC = 0.84 (±0.03) and accuracy = 0.94 (±0.01). XGBoost (AUROC: 0.80±0.04, accuracy: 0.91±0.02) and Extremely Randomized Trees (AUROC: 0.80± 0.03; accuracy: 0.93±0.01) were sufficient as well. SVM (AUROC: 0.55±0.05); accuracy: 0.91±0.01) and KNN (AUROC: 0.49±0.05; Accuracy: 0.74±0.03) performed no better than random chance, however.

Discussion We demonstrate that well-designed models trained on a small dataset can successfully predict non-home discharges in unruptured intracranial aneurysm treatment. Tree-based models (Random Forest, Extremely Randomized Trees, and XGBoost) outperformed SVM and KNN, indicating that future studies may want to consider tree-based models for similar tasks. We prove that our models, and more generally, machine learning, can be used to provide precise and personalized neurosurgical care.

Disclosures S. Patel: None. **K. El Naamani:** None. **A. Hunt:** None. **P. Jain:** None. **C. Lawall:** None. **C. Yudkoff:** None. **O. El Fadel:** None. **M. Ghanem:** None. **P. Mastorakos:** None. **A. Momin:** None. **A. Alhussein:** None. **R. Alhussein:** None. **E. Atallah:** None. **R. Abbas:** None. **R. Zakar:** None. **S. Tjoumakaris:** 2; C; MicroVention. **M. Gooch:** 2; C; Stryker. **N. Herial:** None. **H. Zarzour:** None. **R. Schmidt:** None. **R. Rosenwasser:** None. **P. Jabbour:** 2; C; Medtronic, MicroVention, Balt, Cerus Endovascular.

E-227 DELAYED DIAGNOSIS OF CAROTID CAVERNOUS FISTULA IN PATIENTS WITH OCULAR SYMPTOMS: A CASE SERIES AND LITERATURE REVIEW

[1]M Khasawneh*, [1]A Li, [2]Y Lee, [3]A Vellimana, [2]C Moran. *[1]Neurology, Washington University School of Medicine, Saint Louis, MO; [2]Mallinckrodt Institute of Radiology, Washington University School of Medicine, Saint Louis, MO; [3]Neurosurgery, Washington University School of Medicine, Saint Louis, MO*

10.1136/jnis-2024-SNIS.332

Introduction Carotid-Cavernous Fistulas (CCF) can be diagnostically challenging due to their diverse clinical presentations. Due to its anatomical location and the critical structures housed within the cavernous sinus, patients often present with nonspecific ocular symptoms. These presenting symptoms can mimic other ophthalmic and infectious conditions, leading to initial misdiagnosis. Highlighting this diagnostic complexity, we present a case series of three patients who initially presented

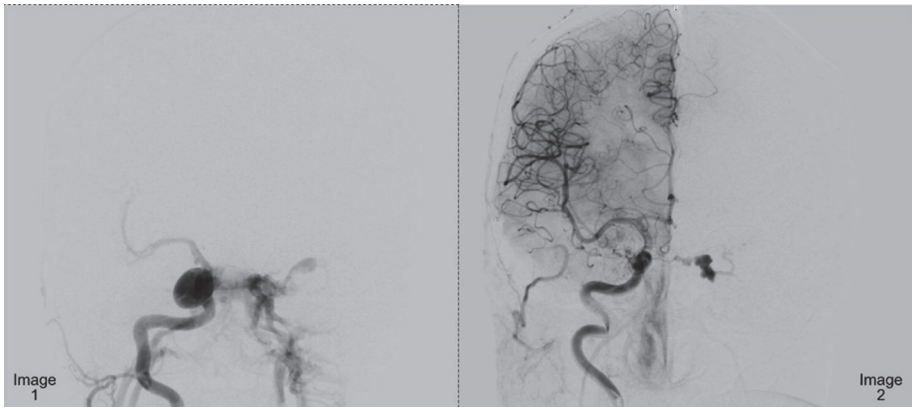

Abstract E-227 Images 1 and 2

with ocular symptoms, ultimately leading to the diagnosis of CCF.

Materials and Methods We conducted a retrospective chart review of our institution's database between December 2022 and February 2024 to identify patients who initially presented with ocular symptoms such as unilateral ocular pain, proptosis, or vision loss. These patients received an initial diagnosis other than CCF but were ultimately diagnosed with CCF.

Results Three patients were identified: Case 1: A 72-year-old woman with worsening vision initially attributed to local spread of dental infection; showed no improvement with antibiotics. DSA revealed a ruptured right cavernous ICA aneurysm (16.7×15.2×14.8 mm) with direct right CCF (bilateral jugular bulb/internal jugular vein drainage). Steal syndrome caused by the fistula led to minimal right cerebral hemisphere perfusion. [Image 1: lateral view of left ICA angiography] Case 2: A 71-year-old woman with periorbital pain and swelling after a dental abscess. Despite initial treatment with antibiotics for presumed orbital cellulitis, she developed proptosis and vision loss. Imaging revealed left cavernous sinus thrombosis and a CCF (Barrow D, bilateral meningeal/external carotid feeders, right superior ophthalmic vein drainage). [Image 2: Anteroposterior view of right ICA angiography] Case 3: A 61-year-old woman with right eye swelling and blurry vision received treatment for a presumed infectious etiology based on MSSA bacteremia (ophthalmic vein thrombosis/cavernous sinus thrombosis/cellulitis). Follow-up imaging suggested right CCF. DSA confirmed a ruptured, partially thrombosed right cavernous ICA mycotic aneurysm (likely CCF source).

Conclusion The presented case series underscores the diverse clinical manifestations and diagnostic challenges associated with CCFs. Prompt recognition and accurate diagnosis are paramount, given the potential for irreversible vision loss and neurological complications if left untreated. Clinical suspicion should remain high, particularly in patients presenting with unilateral eye pain, swelling, and elevated intraocular pressure, as timely intervention can mitigate adverse outcomes. While cerebral angiography remains the gold standard for diagnosis, non-invasive imaging modalities such as CT or MR angiography can serve as valuable initial screening tools.

Disclosures M. Khasawneh: None. **A. Li:** None. **Y. Lee:** None. **A. Vellimana:** None. **C. Moran:** None.

E-228 CLINICAL RESULTS OF THE ANAIS STUDY: MECHANICAL THROMBECTOMY USING THE ANACONDA DEVICE IN COMBINATION WITH A STENT RETRIEVER IN SUBJECTS WITH ACUTE ISCHEMIC STROKE

[1]M Ribo*, [2]J Zamarro, [3]M Terceño, [3]S Bashir, [4]L Gramegna, [4]M Requena, [4]F Diana, [4]E Rivera, [5]M De Dios, [5]D Hernandez, [6]S Snchez, [4]I Galve, [5]A Tomasello. *[1]Neurology, Hospital Vall d'Hebron, Barcelona, Netherlands*; *[2]Radiology, Hospital Virgen de la Arrixaca, Murcia, Spain*; *[3]Neurology, Hospital Josep Trueta, Girona, Spain*; *[4]Neurology, Hospital Vall d'Hebron, Barcelona, Spain*; *[5]Radiology, Hospital Vall d'Hebron, Barcelona, Spain*; *[6]Hospital Vall d'Hebron, Barcelona, Spain*

10.1136/jnis-2024-SNIS.333

Background The ANA Mechanical Thrombectomy (MT) device (Anaconda Biomed, Barcelona) comprised of a self-expanding coated funnel, works in conjunction with a standard stentretriever, and is designed to locally restrict flow and reduce clot fragmentation. The ANAIS Study investigated the performance of the ANA device and which procedural circumstances improve its efficacy.

Methods Prospective, single-arm, multi-center study with blinded outcomes assessment by independent imaging core lab. Patients with anterior circulation stroke undergoing MT were eligible. Primary endpoint was successful reperfusion (eTICI≥2b) within three passes without rescue therapy. Safety endpoint combined symptomatic Intracranial Hemorrhage (sICH) and adverse severe device effects (SADE).

Results 43 subjects were treated in 3 centers: mean age: 70.5 ±13.1 years, median admission National Institutes of Health Stroke Scale 16.0 [12.5–19.5]. Primary endpoint was achieved in 70% (30/43) and 81% (26/32) in the intention to treat (ITT) and per protocol (PP) populations, respectively. The rate of first pass eTICI2c-3 was 44% (19/43) and 56% (18/32) in the ITT and PP populations, respectively. There were no SADE/sICH at 24h (0/43). When the funnel was deployed in C1 segment of the internal carotid artery (ICA) the primary endpoint (ITT: 36%; PP: 57%) was lower than when deployed in the C2/C3 segments (ITT:89%; PP:100%; $p < 0.02$), or in the C4 segment of higher (ITT:71%; PP:77%; $p < 0.01$). Primary endpoint was higher when continuous aspiration was applied from initiation of retrieval maneuver (ITT:81%; TT:92%) as compared to end aspiration only